

1 *Research Article*

2 **Magnesium Potassium Phosphate Compound for** 3 **Immobilization of Radioactive Waste Containing** 4 **Actinide and Rare Earth Elements**

5 **Sergey E. Vinokurov***, **Svetlana A. Kulikova** and **Boris F. Myasoedov**

6 Vernadsky Institute of Geochemistry and Analytical Chemistry of the Russian Academy of Sciences,
7 19 Kosygin st., Moscow 119991, Russia

8 * Correspondence: vinokurov.geokhi@gmail.com; Tel.: +7-495-939-7007

9

10 **Abstract:** The problem of effective immobilization of liquid radioactive waste (LRW) is key to the
11 successful development of nuclear energy. The possibility of using magnesium potassium
12 phosphate (MKP) compound for LRW immobilization on the example of nitric acid solutions
13 containing actinides and rare earth elements (REE), including high level waste (HLW) surrogate
14 solution is considered in the research work. Under the study of phase composition and structure of
15 the MKP compounds obtained by the XRD and SEM methods, it was established that the
16 compounds are composed of crystalline phases - analogues of natural phosphate minerals (struvite,
17 metaankoleite). The hydrolytic stability of the compounds was determined according to the
18 semi-dynamic test GOST R 52126-2003. Low leaching rates of radionuclides from the compound
19 are established, including a differential leaching rate of ^{239}Pu and ^{241}Am - 3.5×10^{-7} and 5.3×10^{-7}
20 $\text{g}/(\text{cm}^2 \cdot \text{day})$. As a result of the research work it was concluded that the MKP compound is
21 promising for LRW immobilization and can become an alternative material combining the
22 advantages of easy implementation of the technology like cementation and the high physical and
23 chemical stability corresponding to a glass-like compound.

24 **Keywords:** magnesium potassium phosphate compound; actinides; rare earth elements; uranium;
25 plutonium; americium; lanthanum; neodymium; immobilization; leaching

26

27 **1. Introduction**

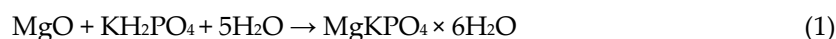
28 Long-term controlled storage or disposal is one of the key stages of the liquid radioactive waste
29 (LRW) management in terms of radiation safety. The preparation of the LRW for this stage involves
30 the transfer of waste into a stable solidified form using preserving matrices [1, 2]. Cementation has
31 found wide use in nuclear industry for radioactive waste (RW) management of low and
32 intermediate activity levels, in spite of significant disadvantages of the method, especially relatively
33 low degree of incorporation of waste salts, as well as low hydrolytic stability and frost resistance of
34 cement compound. Vitrification is currently the only high radioactive waste (HLW) management
35 technology applied in industry [3]. The disadvantages of the method are low chemical and
36 crystallization resistance of the glass at elevated temperatures, as well as the need to use expensive
37 high temperature melters, the liquidation of which, after the end of a relatively short technical
38 lifetime, represents an unresolved radioecological problem.

39 Ceramic materials [4] and especially synthetic analogues of natural phosphate minerals [5,6] are
40 considered as an alternative to cement and glass for the immobilization of RW, primarily obtained
41 after the reprocessing of spent nuclear fuel (SNF) and containing long-lived isotopes of highly toxic
42 actinides and rare earth elements (REE).

43 The mineral-like phosphate materials obtained at room temperature in aqueous solution by
44 chemical interaction, as a rule, between metal (II) oxides (MgO , ZnO , FeO , CaO) and

45 orthophosphoric acid (H_3PO_4) or its derivatives (for example, (di) hydrogenphosphates of metals (I)
46 or ammonium) [7,8] are of particular interest.

47 Previously we and other researchers demonstrated [9-16] that magnesium potassium
48 phosphate (MKP) compound based on the $\text{MgKPO}_4 \times 6\text{H}_2\text{O}$ matrix obtained as a result of the
49 reaction (1), which is an analog of the natural mineral K-struvite [17], is promising low-temperature
50 material for the immobilization of various RW types.



51 This method of RW management combines versatility, equipment simplicity and economic
52 efficiency similar cementation, and the obtained MKP compound has a high physical and chemical
53 stability.

54 The practical use possibility of MKP compound in RW management has to be explained in the
55 context of reliability under long storage of hazardous RW components mainly highly toxic
56 plutonium and minor actinides, as well as REE, whose content is about half the content of all metals
57 in HLW. It should also be noted that although uranium is maximally recovered from solutions
58 during SNF reprocessing for its reuse in the fuel cycle, the residual uranium content (including
59 isotopes U-232, 235, 236, 238) in HLW is about 3 g/L. Thus, information on the behavior of uranium
60 during immobilization in the MKP compound also has scientific interest.

61 The data on the phase composition, structure and hydrolytic stability of synthesized MPP
62 compounds containing uranium, plutonium, americium and REE (on the example, lanthanum and
63 neodymium) are presented in this article.

64 2. Materials and Methods

65 The experiments were performed in the glove box. The chemicals used in the experiments were
66 of no less than chemically pure grade. Samples of MKP compounds were prepared according to the
67 procedure previously given in [10]. To study the forms of location and behavior during leaching of
68 uranium and REE by the example of lanthanum in the MKP compound, concentrated aqueous
69 solutions of their nitrates with a metal concentration 228.3 and 242.4 g/L, respectively, were
70 solidified.

71 The hydrolytic stability of MKP compound to the leaching of actinides and neodymium as a
72 simulator of the REE group was carried out after solidification of the HLW surrogate solution of
73 1000 MW water-water energetic reactor (WWER-1000). The HLW surrogate solution was prepared
74 by dissolving the metal nitrates in an aqueous solution of nitric acid, molybdenum was added in the
75 form of MoO_3 (Table 1). Preparation of the surrogate solution to solidification was carried out by
76 neutralizing it to pH 8.0 ± 0.1 with sodium hydroxide solution at concentration 15.0 ± 0.1 mol/L.

77 **Table 1.** Characteristics of HLW surrogate solution.

Specific activity of actinides, Bq/L	Metal content, g/L	HNO_3 content, mol/L	Density, g/L	Solt content, g/L
$^{239}\text{Pu} - 3.8 \times 10^8$ $^{241}\text{Am} - 5.2 \times 10^7$	Na – 13.3; Sr – 3.9; Zr – 7.6; Mo – 0.9; Pd – 5.4; Cs – 9.3; Ba – 6.4; Nd – 28.8; Fe – 1.0; Cr – 2.8; Ni – 0.5; U – 3.1	3.2	1210	206.6

78 The phase composition and structure of the prepared MKP compounds were determined by
79 X-ray diffraction (XRD) (Ultima-IV, Rigaku). The X-ray diffraction data were interpreted using the
80 specialized Jade 6.5 program package (MDI) with PDF-2 powder database.

81 The structure of samples containing uranium and lanthanum was studied by the scanning
82 electron microscopy (SEM) using microscopes Jeol JSM-6480LV and LEOSupra 50 VP Carl Zeiss,
83 respectively. The electron probe microanalysis of the samples was performed using an
84 energy-dispersive analyzer X-MAX 80 (Oxford Inst.).

85 The hydrolytic stability of compounds was determined using the semidynamic test in
86 accordance with standard [18]. Conditions: monolithic compound 2×2×2 cm; leaching agent -
87 bidistilled water (pH 6.6 ± 0.1, volume 200 mL), temperature 23 ± 2°C, periodic replacement of the
88 leaching agent after 1, 3, 7, 10, 14 and 21 days, the total duration of the test was limited to 28 days.
89 The content of lanthanum, neodymium and uranium in solutions after leaching was determined by
90 inductively coupled plasma atomic emission spectrometry (ICP-AES) (iCAP-6500 Duo, Thermo
91 Scientific), inductively coupled plasma mass spectrometry (ICP-MS) (X Series2, Thermo Scientific)
92 and by spectrophotometry (Cary 100 Scan, Varian), and the content of ²³⁹Pu and ²⁴¹Am - radiometric
93 method with using of the α -spectrometer Alpha Analyst, Canberra.

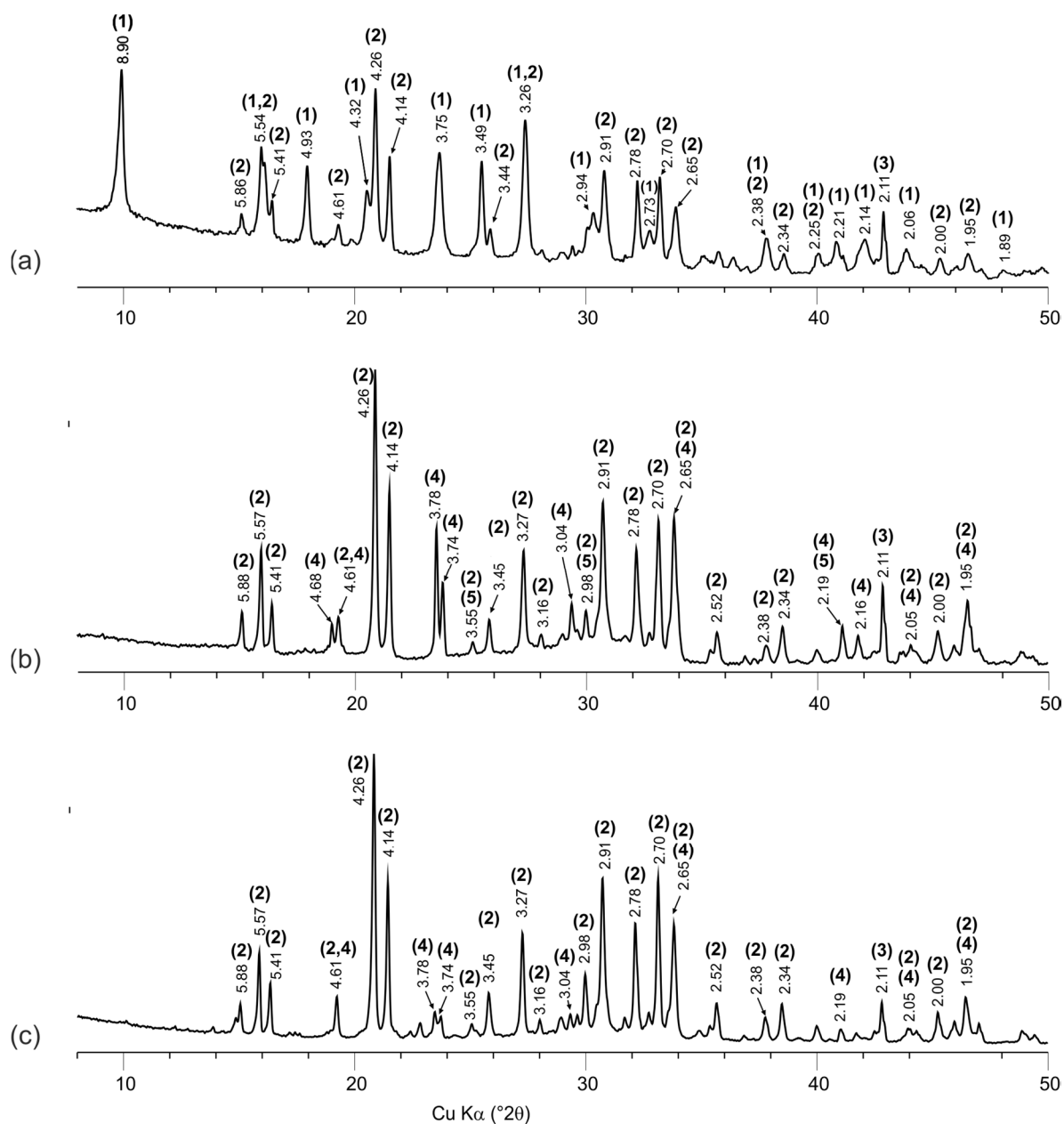
94 The mechanism of leaching of the compound components (lanthanum, neodymium, uranium,
95 plutonium, americium) from the samples was evaluated according to the model [19], described by
96 the linear relationship of $\log(B_i)$ from $\log(t)$, where B_i is the total yield of the element from the
97 compound during contact with water, mg/m²; t is the contact time, days. The calculate procedure of
98 B_i is given in [9, 20]. The following mechanisms of element leaching from the compound correspond
99 to various values of the slope in this equation: >0.65 - surface dissolution; 0.35 - 0.65 – diffusion
100 transport; <0.35 – surface wash off (including with subsequent surface depletion) [9,10,20-23].

101 3. Results

102 As a result of the performed experiments, the samples of MKP compounds with a density of
103 1.75 ± 0.07 g/cm³ were prepared. The content of metals in compounds obtained under solidification
104 of uranium and lanthanum nitrate solutions was 6.2 wt% uranium (hereinafter, compound #1) and
105 6.7 wt% lanthanum (hereinafter, compound #2), respectively. The salt content of the HLW surrogate
106 solution obtained under neutralization was 369.5 g/L, and filling of the compound by the salts of
107 neutralized surrogate solution was 12.8 wt%, and the specific activity of ²³⁹Pu and ²⁴¹Am was 1.8 × 10⁵
108 and 2.4 × 10⁴ Bq/g (hereinafter, compound # 3).

109 The obtained data on the study of the phase composition and structure of synthesized
110 compounds #1 - 3 by XRD and SEM methods are shown in Figures 1 and 2, respectively.

111 In accordance with standard [18], the differential leaching rates of actinides and REE from
112 synthesized compound #1-3 during 28 days of contact with water (Figures 3a, 3c, 3e) were
113 determined, and the mechanisms of their leaching (Figures 3b, 3d, 3f, summarized in Table 2) were
114 estimated.



115

116

117

1 – $K(\text{UO}_2)\text{PO}_4 \times 3\text{H}_2\text{O}$ (metaankoleite); 2 – $\text{MgKPO}_4 \times 6\text{H}_2\text{O}$ (K-struvite); 3 – MgO (periclase);

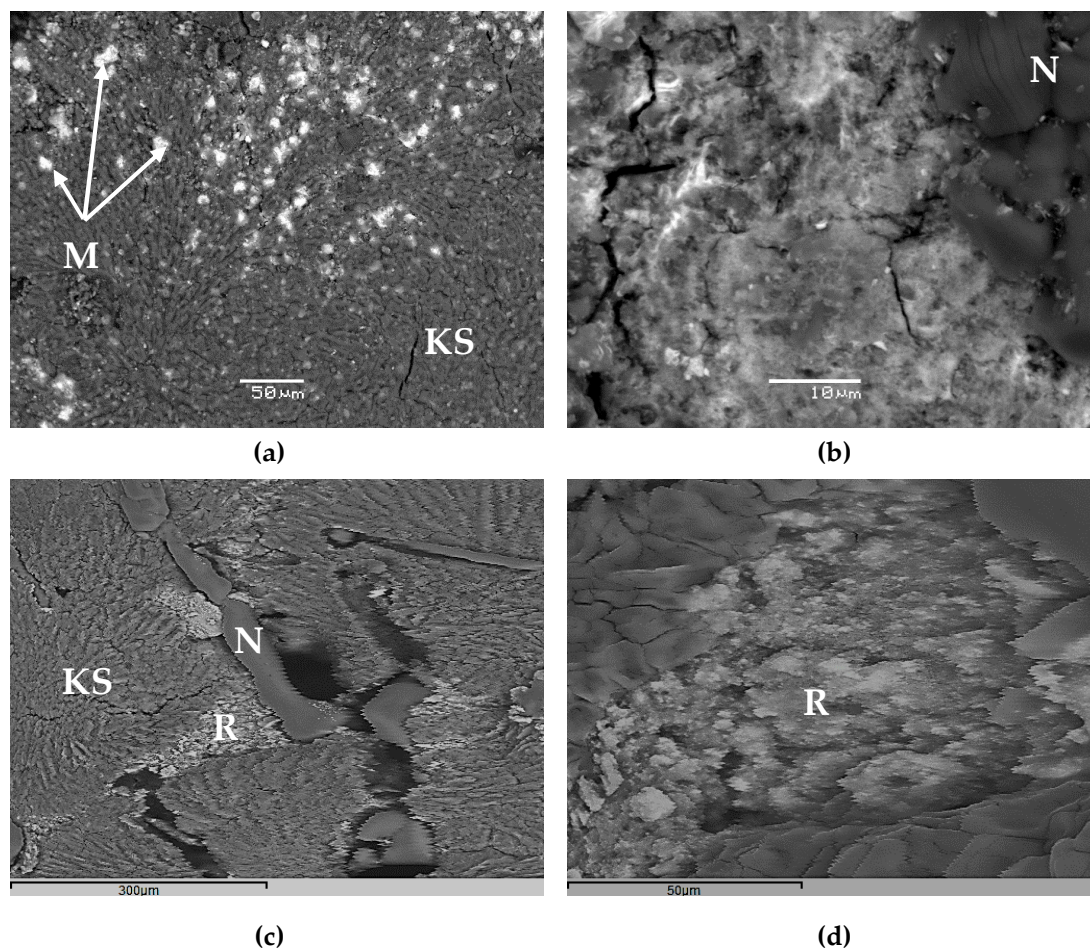
118

119

120

4 – KNO_3 (niter); 5 – $\text{LaPO}_4 \times 0.5\text{H}_2\text{O}$ (rhabdophane-La))

Figure 1. X-ray diffraction patterns of the compounds: #1 (a) and #2 (b), containing 6.2 and 6.7 wt% uranium and lanthanum, respectively, and #3 (c), obtained by solidification of HLW surrogate solution.



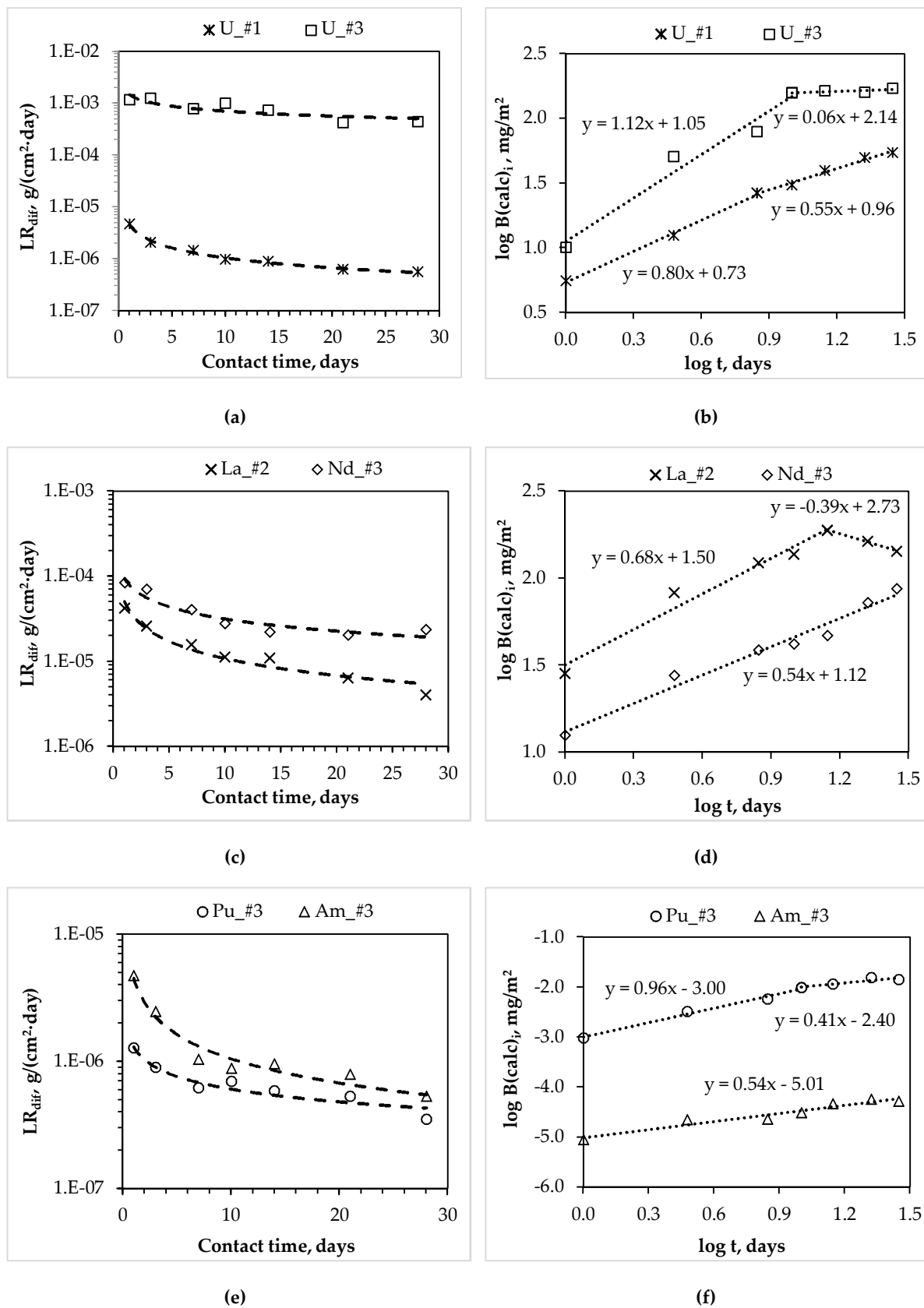
121

M – metaankoleite; *KS* – K-struwoite; *N* – niter; *R* – rhabdophane-(La)

122

Figure 2. SEM images of the compounds #1 (a, b) and #2 (c, d), containing 6.2 and 6.7 wt% uranium and lanthanum, respectively.

123



124
 125
 126

Figure 3. Dependence of the differential leaching rate (LR_{dif}) of actinides and REE (a, c, e) and the logarithmic dependence of their yield ($\log B(\text{calc})$) from compounds (b, d, f) on contact time with water (indices #1, 2, 3 correspond to compounds containing actinides and REE).

127
128**Table 2.** The leaching mechanism of components of the MKP compounds (indices #1, 2, 3 correspond to the names of compounds containing actinides and REE).

Components of the MKP compounds	Correspond figure	Contact time of the samples with water, days	Slope of the lines	Leaching mechanism
U_#1	3b	1-7 7-28	0.80 0.55	dissolution diffusion
U_#3	3b	1-10 10-28	1.12 0.06	dissolution depletion
La_#2	3d	1-14 14-28	0.68 -0.39	dissolution depletion
Nd_#3	3d	1-28	0.54	diffusion
Am_#3	3f	1-28	0.54	diffusion
Pu_#3	3f	1-10 10-28	0.96 0.41	dissolution diffusion

129 **4. Discussion**130 **4.1. Phase composition and structure of MKP compounds**

131 The base of all the studied samples of compounds is the crystalline phosphate phase - the
 132 synthetic analogue of the K-struvite natural mineral $\text{MgKPO}_4 \times 6\text{H}_2\text{O}$ (the characteristic peaks at
 133 4.26, 4.14, 2.91, 2.70 Å) (Figure 1a-1c). In this case, compound #1 also contains a significant amount of
 134 the hydrated potassium uranyl orthophosphate phase, the X-ray diffraction parameters of which
 135 correspond to the metaankoleite mineral $\text{K}(\text{UO}_2)\text{PO}_4 \times 3.0\text{H}_2\text{O}$ (the characteristic peaks at 8.90, 3.75,
 136 3.49 Å) (Figure 1a). This is confirmed by the results of calculating the compound #1 phase
 137 composition according to the microanalysis data: the uranium-enriched particles (denoted by M in
 138 Figure 2a) contain up to 45 wt% of uranium and have an average composition $\text{Mg}_{0.33}\text{K}(\text{UO}_2)_{0.67}\text{PO}_4 \times$
 139 $4.0\text{H}_2\text{O}$, which corresponds to a mixture of metaankoleite $\text{K}(\text{UO}_2)\text{PO}_4 \times 3.0\text{H}_2\text{O}$ and the K-struvite
 140 $\text{MgKPO}_4 \times 6.0\text{H}_2\text{O}$ in a molar ratio of 2/1. In this case, the main phase of compound #1 (phase KS in
 141 Figure 2a) contains up to 3 wt% of uranium.

142 As a result of potassium replacement with metals of nitric acid solutions, the KNO_3 (niter)
 143 phase (the characteristic peaks at 3.78, 3.74, 3.04 Å) is formed in the obtained compounds (Figure 1),
 144 that was also shown previously in [9, 10]. However, it was not possible to identify this phase in
 145 compound #1 (Figure 1a) by XRD method, probably because of its small content (theoretically not
 146 more than 5 wt%), but its presence is clearly confirmed by microanalysis data (phase N in Figure 2b).
 147 Impurities of magnesium, phosphorus and uranium in phase N (Figure 2b) don't exceed 0.6, 1.4 and
 148 1.3 wt%, respectively.

149 According to XRD (Figure 1b) and SEM (R in Figure 2c, d), it was established that lanthanum as
 150 REE in compound #2 is present as a phosphate compound of the analogue of the natural mineral
 151 rhabdophane - (La) $\text{LaPO}_4 \times 0.5\text{H}_2\text{O}$. In this case, according to the microanalysis data, the main phase
 152 of compound #2 (phase KS Figure 2c) is a phosphate compound of the composition
 153 $\text{Mg}_{0.60}\text{K}_{0.68}\text{La}_{0.36}\text{PO}_4 \times 6.3\text{H}_2\text{O}$, similar to K-struvite. In compound #2, SEM data also unambiguously
 154 confirmed the presence of the KNO_3 phase (N in Figure 2c). In compound #2, the presence of the
 155 KNO_3 phase (N in Figure 2c) is also clearly confirmed by SEM data.

156 The MgO (periclase) phase (the characteristic peak at 2.11 Å) is present in all studied
157 compounds (Figure 1), and it is associated with an excess of the 10 wt% used MgO relative to the
158 stoichiometry of the reaction (1) in accordance with the technique [10].

159 4.2. The leaching rate and mechanism of actinides and REE from MKP compounds

160 The leaching rate of all metals decreases depending on the contact time of the studied
161 compounds with water (Figure 3a, c, e). However, a significant difference in the rate of uranium
162 leaching from compounds #1 and #3 was established: at 28th day, the differential uranium leaching
163 rate is 5.5×10^{-7} and 4.4×10^{-4} g/(cm²·day), respectively (Figure 3a). It was determined by XRD and
164 SEM (Figures 1a and 2a) that uranium in compound #1 is bound in a slightly soluble phosphate,
165 which is analog of the natural mineral metaankoleite [24, 25], which provides a high resistance of
166 compound #1 to uranium leaching. Obviously, the formation of such stable phase did not occur
167 under the high-salt HLW surrogate solution solidification in compound #3, due to the presence of a
168 large amount of nitrates of various metals (salt background - 369.5 g/L).

169 Data on the uranium leaching mechanism from compounds #1 and #3 (Figure 3b, Table 2)
170 confirm the difference in leaching behavior. The logarithmic dependence of the uranium yield from
171 compound #1 on the time of contact with water can be divided into 2 sections, which are described
172 by linear equations with the slopes are 0.80 and 0.55 for 7 days from the beginning of the test and the
173 next 21 days, respectively. Thus, the uranium leaching mechanism varies depending on the duration
174 of contact of the compound with water. So, during the first 7 days uranium leaching occurs due to
175 surface dissolution of the compound, where individual particles of hydrated uranyl nitrate were
176 localized. In the next 21 days, the uranium leaching is precisely determined by the diffusion
177 transport from the inner layers of the compound. The uranium leaching from compound #3 in the
178 first 10 days is determined by the intensive surface dissolution, which is probably enriched by
179 uranyl nitrate, and in the next 18 days - due to the gradual surface depletion (the slopes are 1.12 and
180 0.06, respectively).

181 The leaching rate of trivalent REE from the MKP compound increases with the increasing of
182 content of various salts in the compound (for example, lanthanum and neodymium, Figure 3c). So
183 for compounds #2 and #3 the differential leaching rate of REE on the 28th day is 4.1×10^{-6} g/(cm²·day)
184 for lanthanum from compound #2, and 2.4×10^{-5} g/(cm²·day) for neodymium from compound #3. It
185 is obvious (Figure 3d) that under contact of compound #2 with water, the lanthanum leaching rate
186 will decrease, since lanthanum leaching for 14 days is probably due to the surface dissolution (slope
187 = 0.68) of soluble lanthanum forms of compound #2 in consequence of significant its content in the
188 compound (6.2 wt%) with the next surface depletion (slope = -0.39). It is important to note that the
189 neodymium leaching from compound #3 is uniquely determined by diffusion from the inner layers
190 of the compound (slope = 0.54), which probably contains a uniformly distributed phase of hydrated
191 neodymium nitrate unbound in slow-soluble phosphate forms.

192 The ²³⁹Pu leaching rate is the main criterion of matrix quality evaluation for HLW
193 immobilization. It has been established that compound #3 reliably kept both plutonium and
194 americium: the differential leaching rate of ²³⁹Pu and ²⁴¹Am on 28th day is 3.5×10^{-7} and 5.3×10^{-7}
195 g/(cm²·day), respectively (Figure 3e). The plutonium yield from compound #3 in the leaching agent
196 in the first 10 days occurred under the surface dissolution of the compound (slope = 0.96), and then
197 by diffusion transport (slope = 0.41, Figure 3f). Americium leaching is also determined by diffusion
198 transport (slope = 0.54), probably from the slow-soluble mixed orthophosphate (Am, REE)PO₄,
199 which is analogue of the natural mineral monazite.

200 The established low value of the ²³⁹Pu leaching rate from MKP compound is close to the
201 standard requirements for the glass-like compound for HLW immobilization (1×10^{-7} g/(cm²·day)).
202 However, it is important to note that MKP compound is synthesized at room temperature, whereas
203 vitrification requires the use of expensive high-temperature electric furnaces or special melters, the
204 liquidation of which after the end of the service life is a great radioecological problem, which yet
205 unsolved. Thus, the MKP compound approbation for immobilization of real wastes samples
206 obtained by radiochemical plants during reprocessing of SNF, and a systematic comparison of MKP

207 and glass-like compound quality indicators, including taking into account the technical and
208 economic evaluation of these technologies, are of scientific interest.

209 5. Conclusions

210 As a result of the research, it was established that MKP compounds synthesized at room
211 temperature under solidification of nitric acid solutions, which are the surrogate solution of LRW,
212 having complex chemical composition and containing actinides and REE, consist of crystalline
213 phases - analogues of natural phosphate minerals and possess high hydrolytic stability. Thus, MKP
214 compound is promising for the immobilization of LRW and can be an alternative material
215 combining the advantages of technology implementation simplicity similar to cementation and high
216 physical and chemical stability corresponding to the glass-like compound.

217 **Acknowledgments:** The study was carried out through the Russian Science Foundation grant (project No
218 16-13-10539).

219 **Author Contributions:** S.E. Vinokurov and B.F. Myasoedov conceived and designed the experiments; S.E.
220 Vinokurov and S.A. Kulikova performed the experiments; S.E. Vinokurov, S.A. Kulikova and B.F. Myasoedov
221 wrote the paper.

222 **Conflicts of Interest:** The authors declare no conflict of interest. The founding sponsors had no role in the
223 design of the study; in the collection, analyses, or interpretation of data; in the writing of the manuscript, and in
224 the decision to publish the results.

225 References

- 226 1. Ojovan, M.I.; Lee, W.E. *An Introduction to Nuclear Waste Immobilisation*, 2nd ed.; Elsevier, Netherlands, 2014;
227 pp. 1-362, ISBN: 978-0-08-099392-8.
- 228 2. Stefanovsky, S.V.; Yudintsev, S.V.; Vinokurov, S.E.; Myasoedov, B.F. Chemical-technological and
229 mineralogical-geochemical aspects of the radioactive waste management. *Geochem. Int.* **2016**, *54*, 1136-1156,
230 DOI: 10.1134/S001670291613019X.
- 231 3. Stefanovsky, S.V.; Stefanovskaya, O.I.; Vinokurov, S.E. et al. Phase composition, structure, and hydrolytic
232 durability of glasses in the Na₂O-Al₂O₃-(Fe₂O₃)-P₂O₅ system at replacement of Al₂O₃ by Fe₂O₃. *Radiochem.*
233 **2015**, *57*, 348-355, DOI: 10.1134/S1066362215040037.
- 234 4. Ewing, R.C.; Lutze, W.F. High-level nuclear waste immobilization with ceramics. *Ceramics Int.* **1991**, *17*,
235 287-293, DOI: 10.1016/0272-8842(91)90024-T.
- 236 5. Schlenz, H.; Neumeier, S.; Hirsch, A. et al. Phosphates as safe containers for radionuclides. In *Highlights in*
237 *Applied Mineralogy*; Heuss-Aßbichler, S., Amthauer, G., John, M., Eds.; De Gruyter, Germany, 2017; pp.
238 171-196, ISBN 9783110497342.
- 239 6. Schlenz, H.; Heuser, J.; Neumann, A. et al. Monazite as a suitable actinide waste form. *Z. Kristallogr. Cryst.*
240 *Mater.* **2013**, *228*, 113-123, DOI: 10.1524/zkri.2013.1597.
- 241 7. Wagh, A.S. *Chemically Bonded Phosphate Ceramics: Twenty-First Century Materials with Diverse Applications*,
242 2nd ed.; Elsevier, Netherlands, 2016, pp. 1-422, ISBN: 978-0-08-100380-0.
- 243 8. Roy, D.M. New Strong Cement Materials: Chemically Bonded Ceramics. *Science* **1987**, *235*, 651-658.
- 244 9. Vinokurov, S.E.; Kulikova, S.A.; Krupskaya, V.V. et al. Investigation of the leaching behavior of
245 components of the magnesium potassium phosphate matrix after high salt radioactive waste
246 immobilization. *J. Radioanal. Nucl. Chem.* **2018**, *315*, 481-486, DOI: 10.1007/s10967-018-5698-3.
- 247 10. Vinokurov, S.E.; Kulikova, S.A.; Krupskaya, V.V.; Myasoedov, B.F. Magnesium Potassium Phosphate
248 Compound for Radioactive Waste Immobilization: Phase Composition, Structure, and Physicochemical
249 and Hydrolytic Durability. *Radiochem.* **2018**, *60*, 70-78, DOI: 10.1134/S1066362218010125.
- 250 11. Myasoedov, B.F.; Kalmykov, S.N.; Kulyako, Yu.M.; Vinokurov, S.E. Nuclear fuel cycle and its impact on
251 the environment. *Geochem. Int.* **2016**, *54*, 1156-1167, DOI: 10.1134/S0016702916130115.
- 252 12. Vinokurov, S.E.; Kulyako, Yu.M.; Slyunchev, O.M. et al. Low-temperature immobilization of actinides and
253 other components of high-level waste in magnesium potassium phosphate matrices. *J Nuclear Materials*
254 **2009**, *385*, 189-192, DOI: 10.1016/j.jnucmat.2008.09.053.
- 255 13. Vinokurov, S. E.; Kulyako, Yu. M.; Slyunchev, O. M. et al. Magnesium potassium phosphate matrices for
256 immobilization of high-level liquid wastes. *Radiochem.* **2009**, *51*, 65-72, DOI: 10.1134/S1066362209010159.

- 257 14. Wagh, A.S.; Sayenko, S.Y.; Shkuropatenko, V.A. et al. Experimental study on cesium immobilization in
258 struvite structures. *J. Hazard. Mater.* **2016**, *302*, 241-249, DOI: 10.1016/j.jhazmat.2015.09.049.
- 259 15. Wagh, A.S.; Strain, R.; Jeong, S.Y. et al. Stabilization of Rocky Flats Pu-contaminated ash within chemically
260 bonded phosphate ceramics. *J. Nucl. Mater.* **1999**, *265*, 295-307, DOI: 10.1016/S0022-3115(98)00650-3.
- 261 16. Singh, D.; Mandalika, V.R.; Parulekar, S.J.; Wagh, A.S. Magnesium potassium phosphate ceramic for ⁹⁹Tc
262 immobilization. *J. Nucl. Mater.* **2006**, *348*, 272-282, DOI: 10.1016/j.jnucmat.2005.09.026.
- 263 17. Graeser, S.; Postl, W.; Bojar, H.-P. et al. Struvite-(K), KMgPO₄·6H₂O, the potassium equivalent of struvite –
264 a new mineral. *Eur. J. of Mineral.* **2008**, *20*, 629-633, DOI: 10.1127/0935-1221/2008/0020-1810.
- 265 18. GOST R 52126-2003. *Radioactive waste. Long time leach testing of solidified radioactive waste forms*. Gosstandart
266 of Russia, Moscow, 2003; pp. 1-8.
- 267 19. de Groot, G.J.; van der Sloot, H.A. Determination of leaching characteristics of waste materials leading to
268 environmental product certification. In *Stabilization and solidification of hazardous, radioactive and mixed*
269 *wastes*; Gilliam, T.M., Wiles, G., Eds.; ASTMSTP 1123, Philadelphia, American Society for Testing and
270 Materials, 1992; Vol. 2, pp.149-170, DOI: 10.1520/STP19548S.
- 271 20. Torras, J.; Buj, I.; Rovira, M.; de Pablo, J. Semi-dynamic leaching tests of nickel containing wastes
272 stabilized/solidified with magnesium potassium phosphate cements. *J. Hazard. Mater.* **2011**, *186*, 1954-1960,
273 DOI: 10.1016/j.jhazmat.2010.12.093.
- 274 21. Al-Abed, S.R.; Hageman, P.L.; Jegadeesan, G. et al. Comparative evaluation of short-term leach tests for
275 heavy metal release from mineral processing waste. *Sci. Total Environ.* **2006**, *364*, 14-23, DOI:
276 10.1016/j.scitotenv.2005.10.021.
- 277 22. Moon, D.H.; Dermatas, D. An evaluation of lead leachability from stabilized/solidified soils under
278 modified semi-dynamic leaching conditions. *Eng. Geol.* **2006**, *85*, 67-74, DOI: 10.1016/j.enggeo.2005.09.028.
- 279 23. Xue, Q.; Wang, P.; Li, J.-S. et al. Investigation of the leaching behavior of lead in stabilized/solidified waste
280 using a two-year semi-dynamic leaching test. *Chemosphere* **2017**, *166*, 1-7, DOI:
281 10.1016/j.chemosphere.2016.09.059.
- 282 24. Gallagher, M.J.; Atkin, D. Meta-ankoleïte, hydrated potassium uranyl phosphate. *Bull. Geol. Soc. Great*
283 *Britain.* **1966**, *25*, 49-54.
- 284 25. Fleischer, M. New mineral names. *Am. Mineral.* **1967**, *52*, 559-564.